Proceedings of the 26th International Conference on Offshore Mechanics and Arctic Engineering
OMAE2007
June 10-15, 2007, San Diego, California, USA

OMAE2007-29327

EMPIRICAL WIND TURBINE LOAD DISTRIBUTIONS USING FIELD DATA

P. Agarwal
Dept. of Civil, Arch., and Env. Engineering
University of Texas
Austin, TX 78712, USA
Email: pagarwal@mail.utexas.edu

L. Manuel
Dept. of Civil, Arch., and Env. Engineering
University of Texas
Austin, TX 78712, USA
Email: lmanuel@mail.utexas.edu

ABSTRACT

In the design of land-based or offshore wind turbines for ultimate limit states, long-term loads associated with return periods on the order of the service life (20 years, usually) must be estimated. This requires statistical extrapolation from turbine loads data that may be obtained by simulation or by field tests. The present study illustrates such extrapolation that uses field data from the Blyth offshore wind farm in the United Kingdom, where a 2MW wind turbine was instrumented, and environment and loads data were recorded. From this measurement campaign, the loads data available are in two different formats: as ten-minute statistics (referred to as "summary" data) and as full time series (referred to as "campaign" data). The characteristics of the site and environment and, hence, of the turbine response as well are strikingly different for wind regimes associated with onshore winds (winds from sea to land) and offshore winds (those from land to sea). The loads data (here, only the mudline bending moment is studied) at the Blyth site are hence separated depending on wind regime. By integrating load distributions conditional on the environment with the relative likelihood of the different environmental conditions, long-term loads associated with specified return periods can be derived. This is achieved here using the peak-over-threshold method based on campaign data but derived long-term loads are compared with similar estimates based on the summary data. Offshore winds are seen to govern the long-term loads at the site. Though the influence of wave heights on turbine long-term loads is smaller than that of wind speed, there is possible resonance of tower dynamics induced by the waves; still, to first order, it is largely the wind speed and turbulence intensity that control the design loads. Predicted design loads based on the campaign data are close to those based on the summary data discussed in a separate study.

INTRODUCTION

Our objective is to estimate design loads for an offshore wind turbine for which the environmental and load data are available from field measurements. Using a probabilistic approach, we intend to estimate design loads associated with a target failure probability or, equivalently, a prescribed service life for the turbine. Variables describing the wind and wave environment as well as the turbine response are modeled as random; their probabilistic distributions need to be established. Available data obtained from full-scale field measurements can provide a more realistic representation of the turbine response subjected to various environmental conditions than is possible with simulation data. Field data, however, can be "limited" in the sense that they are often recorded only for a finite period of time, and may not systematically cover all the possible environmental conditions expected to occur over the life of the turbine. Hence, with such limited data, statistical techniques are often used to extrapolate the loads from observed events to rarer loads associated with prescribed safety levels. Statistical extrapolation has been used to predict both extreme and fatigue design loads for wind turbines. A recent draft from the International Electrotechnical Commission (IEC) [1] of offshore wind turbine design guidelines also recommends its use. Examples of its use in other studies related to wind turbine loads include those by Moriarty et al [2], Fitzwater and Winterstein [3], and Agarwal and Manuel [4].

Our focus here is on the bending moment at the base of the turbine tower (the mudline bending moment) as the load variable of interest. The turbine under consideration is an instrumented 2MW wind turbine at the Blyth wind farm, located about one kilometer off the northeast coast of England, and for which data were recorded for about sixteen months. Key features of the site pertinent to the present study include contrasting characteristics of the environment and

response associated with winds blowing from the shore to the sea (offshore winds) versus those associated with winds blowing from the sea to the shore (onshore winds). We use the campaign data (available as ten-minute time series) to predict long-term design loads. To gain a better understanding, we separate the data into offshore and onshore wind regimes as well as divide the data in each regime according to ten-minute average wind speed, V, and significant wave height, H_s. Then, for each bin or interval representing different V-H_s combinations, "short-term" load extreme probability distributions are derived using the peak-over-threshold (POT) method. Integration of these short-term load distributions with the likelihood of different V-H_s combinations in the offshore and onshore environments can help to derive the desired design load. Due to statistical uncertainty associated with the use of limited data, we discuss how non-parametric bootstrap methods can be used to establish confidence intervals on design load predictions. The results from this study based on POT data are compared with those from a separate study that employed global (or epochal) load maxima available from summary data.

LOAD EXTRAPOLATION

Design Load Case 1.1b of the IEC 61400-3 draft design guidelines recommends the use of statistical extrapolation methods to predict extreme turbine loads [1]. With statistical extrapolation for wind turbine extreme loads, one seeks to estimate the turbine design load, l_T, associated with an acceptable failure probability, P_T, or equivalently with a target service life of T years, using the following equation:

$$P_T = P[L > l_T] = \int_{\boldsymbol{X}} P[L > l_T \mid \boldsymbol{X} = \boldsymbol{x}] f_{\boldsymbol{X}}(\boldsymbol{x}) d\boldsymbol{x} \qquad (1)$$

where $f_{\boldsymbol{X}}(\boldsymbol{x})$ is the joint probability density function (PDF) of the environmental random variables, $\boldsymbol{X}$. For different trial values of load, l_T, Eq. (1) enables one to compute the long-term probability of exceeding that load by integrating the short-term load exceedance probability conditional on $\boldsymbol{X}$, namely $P[L > l_T \mid \boldsymbol{X} = \boldsymbol{x}]$, with the relative likelihood of different environmental conditions, $\boldsymbol{X}$. One is required to integrate over the entire domain of all random variables; the load level, l_T, is adjusted until the target probability, P_T, results from the integration. In this study, the environmental random variables taken to comprise $\boldsymbol{X}$ are the ten-minute mean wind speed, V, at hub height in the along-wind direction and the significant wave height, H_s. The short-term load distribution, $P[L > l_T \mid \boldsymbol{X} = \boldsymbol{x}]$, is established for different values of $\boldsymbol{X}$ by applying the POT method to the available campaign data time series.

THE BLYTH SITE AND FIELD DATA

The Blyth project is an experimental wind farm consisting of two 2MW Vestas V66 wind turbines. The site is located on the northeast coast of England, off the Northumberland shore. The turbines are located approximately 1 km from the shoreline. The mean water depth at the instrumented turbine varies between a Lowest Astronomical Tide (LAT) level of 6 m and a Mean High Water Springs (MHWS) level of 11 m.; the average water depth is approximately 9 m. One of the two turbines (the southern turbine in Fig. 1(a)) at Blyth was instrumented as part of a research project funded by the European Commission; it has a hub height of 62 m above the LAT level and a blade diameter of 66 m. The turbines are located on sharply sloping submerged rock, known as the 'North Spit,' in rock-socket type foundations.

Field measurements were collected for sixteen months between October 2001 and January 2003, thus covering more than one full winter season. Measured data included wind speed and direction at the nacelle, sea surface elevation, and bending moments at several vertical stations along the tower and the pile. One of these stations—the mudline bending moment—is our load variable of interest here. Figure 1(b) shows the layout of the turbine instrumentation. Additional details regarding the data and measurement system may be found in the report by Camp et al [5].

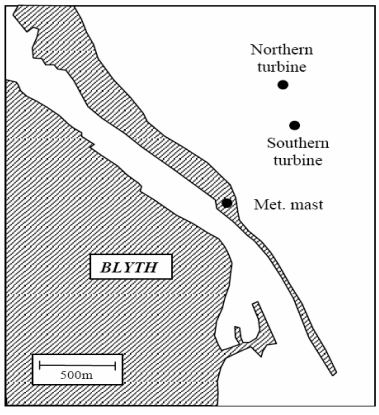

(a)

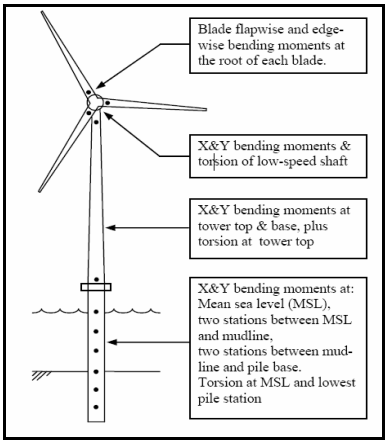

(b)

Figure 1. (a) Location of the turbines and an onshore meteorological mast at the Blyth site; (b) Layout of the turbine instrumentation (from Camp et al [5]).

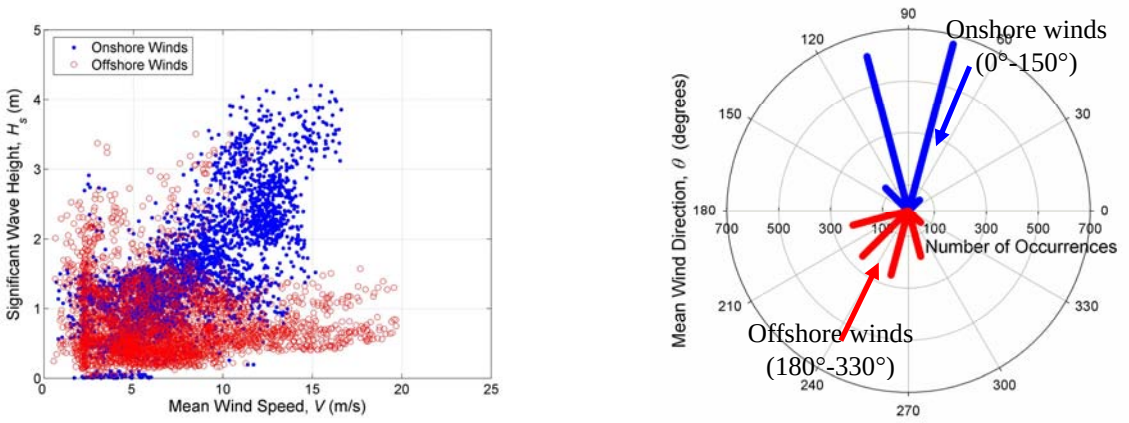

Figure 2: (a) Scatter diagram showing mean wind speed versus significant wave heights and (b) wind-rose.

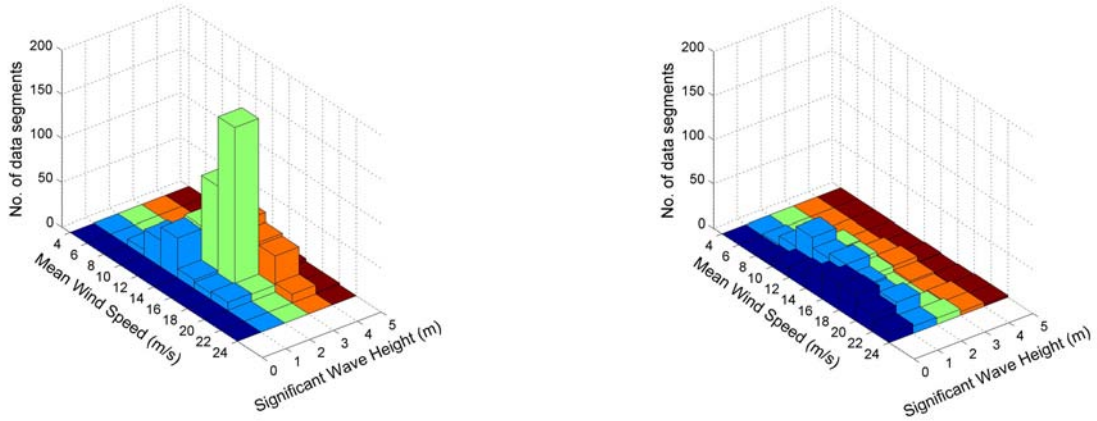

(a) (b)

Figure 3. Distribution of usable campaign data sets by mean wind speed and significant wave height bins for (a) onshore winds and (b) offshore winds.

The joint PDF of $\boldsymbol{X}$ (V and H_s here) needed for the statistical extrapolation is the same as was used by Agarwal and Manuel [4]; a Rayleigh distribution for V (truncated below cut-in and above cut-out wind speeds so as to focus only on the turbine's operating state) and a two-parameter Weibull distribution for H_s given V are assumed. Figure 2(a) shows that, at this site, V and H_s are correlated to different degrees for offshore and onshore winds and that onshore waves are generally higher; also, the wind rose in Fig. 2(b) shows the relatively likelihood of offshore versus onshore winds and the distribution of available data according to wind direction for each wind regime. All of the information in Figs. 2(a) and 2(b) are employed in establishing $f_{\boldsymbol{X}}(\boldsymbol{x})$.

As part of the campaign data, time series for turbine loads in ten-minute segments sampled at 40 Hz were recorded when a predetermined set of trigger conditions were met. In addition, minimum, maximum, mean, and standard deviation values for each channel were recorded as part of the statistics comprising the "summary" data sets (studied by Agarwal and Manuel [4]). The distribution of the usable data of the two types is summarized in Table 1. Figure 3 shows the distribution of the available campaign data according to mean wind speed and significant wave height for onshore and offshore winds.

Table 1: Number of usable ten-minute summary data sets and ten-minute campaign data sets from the Blyth campaign.

Data Type	Onshore Winds	Offshore Winds	All-direction Winds
Summary	1,398	903	2,301
Campaign	646	368	1,014

REPRESENTATIVE SHORT-TERM RESPONSE

We are interested in the response of the turbine while it is in an operating state as a function of wind speed and wave height for onshore and offshore winds. Here, we select one time series each for the offshore and onshore wind directions, for which the largest mudline bending moment was recorded; these are referred to as OffV18H0N1 and OnV12H3N41, respectively. Statistics for the wind, waves, and mudline bending moment for these time series are summarized in Table 2 (one additional time series, referred to as OffV18H0N9, is also discussed in the table for comparison purposes).

Table 2: Statistics of the environment and load time series for the three selected campaigns shown in Fig. 4. (Note: SD: Standard deviation, H_s: Significant wave height.)

Selected time series	Wind speed (m/s)				Sea Surface Elevation	Mudline Bending Moment	
	Nacelle		Met. Mast				
	Mean	SD	Mean	SD	H_s (m)	Extreme (MN-m)	Peak PSD ord. ((MN-m)^2/Hz)
OffV18H0N1	19.1	4.0	15.5	3.6	0.64	23.3	29.3
OffV18H0N9	18.6	2.4	13.9	2.2	0.64	14.9	4.2
OnV12H3N41	13.2	1.8	12.7	1.7	3.47	19.4	1.0

Table 2 shows that the ten-minute extreme mudline bending moments are 23.3 and 19.4 MN-m for the time series, OffV18H0N1 and OnV12H3N41, respectively. The largest load during the campaign was recorded for offshore winds. It is also found that turbine loads are primarily influenced by wind speed and only very slightly by wave height variation. It can be seen from Table 2 that the mean wind speed recorded at the nacelle for time series, OffV18H0N1 and OnV12H3N41, are 19.1 and 13.2 m/s, respectively. Both these mean wind speeds are above the rated wind speed of 12 m/s for this turbine. More interesting is the difference in the standard deviations of the wind speed for these two time series. The turbulence standard deviation for the campaign OffV18H0N1 is more than twice the value observed for the campaign OnV12H3N41. We point out here that wind speed measurements at the nacelle are likely affected by the turbine wake. Only the mean wind speed from the nacelle data was corrected for the free-field mean wind speed (Camp et al [5]); hence, the turbulence standard deviation at the nacelle may not give an accurate estimate of the true turbulence intensity at hub height. Hence, we also compare turbulence standard deviations from another measurement of wind speed at a meteorological mast (met. mast) located on the shore (Fig. 1a). These measurements were, however, taken at a height of 40 m, which is lower than the hub height of 62 m, and also this met. mast is about 1 km away from the turbine. Still, if either the nacelle or the met. mast data are considered, the offshore data segment (OffV18H0N1) is seen to have 50-70% more turbulence intensity than is seen in the onshore data segment (OnV12H3N41). Since turbulence intensity will directly influence turbine loads, we might expect then that the largest loads will result during offshore wind conditions and will likely occur for higher wind speeds there. Evidently, the higher significant wave height for OnV12H3N41 compared to that for OffV18H0N1 has a smaller effect on turbine loads.

Figure 4 shows time series and power spectral density (PSD) functions for the wind speed data (from both nacelle and met. mast), the sea surface elevation, and the mudline bending moment for the three selected time series. For the time series, only a 200-second segment is shown during which the largest load was recorded in each case. As expected, the nacelle turbulence time series and power spectra show more high-frequency content than is seen from the met. mast data; this is probably due to turbine wake effects. Comparing Figs. 4(a) and 4(b)—both for offshore winds—it is seen that for these two time series with comparable mean wind speeds, turbine loads are higher when the turbulence intensity is higher (thus, OffV18H0N1 in Fig. 4(a) has higher loads than OffV18H0N9 in Fig. 4(b)). Both OffV18H0N1 and OffV18H0N9 have comparable significant wave heights and both also have comparable sea surface elevation PSD peaks at the tower natural frequency (approximately 0.5 Hz); clearly, since OffV18H0N1 has the larger turbulence intensity, wind is the more important contributor to turbine loads than waves. Still, resonant vibrations of the tower are at least somewhat contributed to by waves as is clear from studying Fig. 4(a)—for example, the largest loads in the mudline bending moment time series are recorded between 150 and 200 seconds where the load process is oscillating at a frequency of around 0.5 Hz or a period of 2 seconds where waves provide some energy. To summarize, for the two offshore wind cases, the OffV18H0N1 case where the turbulence standard deviation is 3.6 m/s (at the met. mast) compared to 2.2 m/s for the OffV18H0N9 case, experiences the larger load of 23.3 MN-m compared to 14.9 MN-m in the other case.

Figure 4(c) shows similar time series and PSD estimates for an onshore wind data segment, OnV12H3N41, as were studied in Figs. 4(a) and 4(b) for offshore cases. The largest recorded load for onshore winds occurred for the selected data segment. As was discussed earlier, onshore winds are less turbulent than offshore winds; here, for example, turbulence standard deviations are only 1.7 m/s at the met. mast compared to the values of 3.6 m/s and 2.2 m/s, respectively, for the offshore cases, OffV18H0N1 and OffV18H0N9. As a result, despite the fact that the significant wave height for OnV12H3N41 is considerably larger than for OffV18H0N1, the extreme turbine loads are smaller for this offshore case (19.4 MN-m) compared to 23.3 MN-m for OffV18H0N1. Again, we reiterate that turbulence has primary influence on turbine loads and waves have only secondary influence.

While only three ten-minute time series were selected here to illustrate differences between onshore and offshore winds and their influence on turbine loads, the conclusions reached from studying these—namely that offshore winds cause larger loads due to their higher turbulence intensities and that wind speed is more important than wave height—are supported when one studies other data segments in the campaign as well. Next, we derive turbine long-term loads based on short-term extreme load distributions based on POT analyses of all the available time series data.

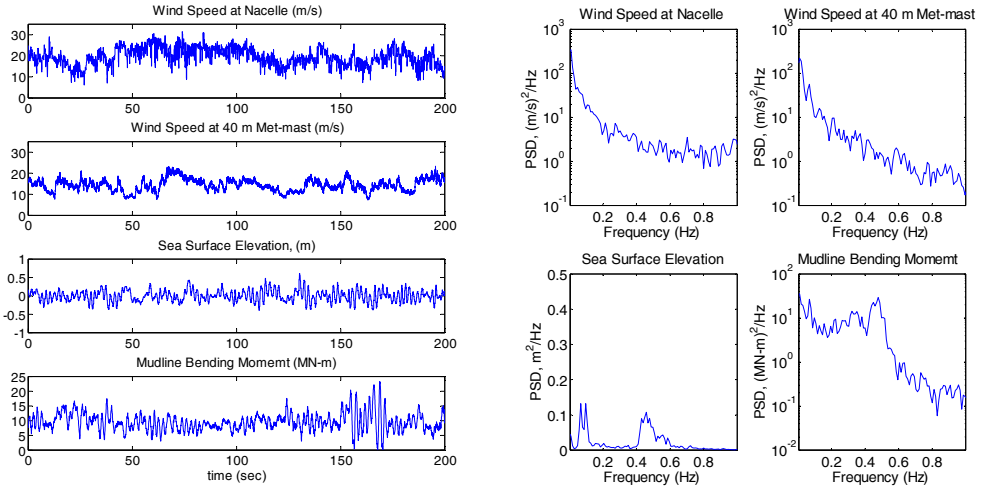

(a)

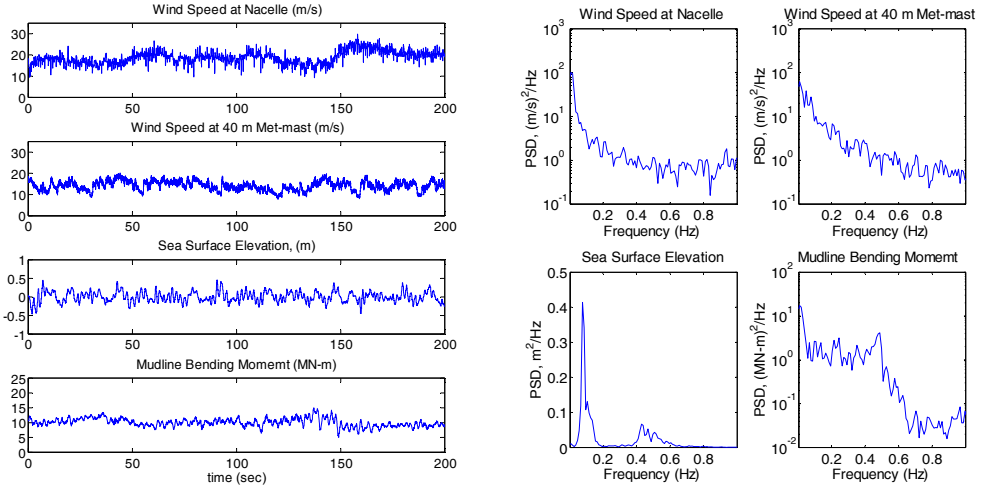

(b)

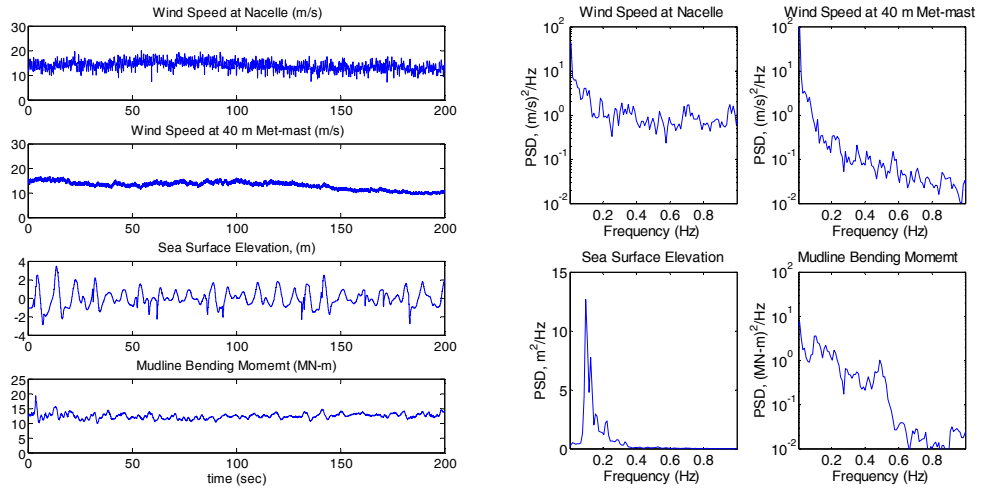

(c)

Figure 4: Time series and power spectra of the wind speed at the nacelle and meteorological mast, the sea surface elevation, and the mudline bending moment for the following ten-minute time series: (a) OffV18H0N1, (b) OffV18H0N9, and (c) OnV12H3N41. Only a 200-second portion is shown for each time series where the maximum load was recorded.

LONG-TERM TURBINE LOADS

Based on Eq. (1), we now discuss derivation of long-term design loads based on first establishing short-term (conditional) distributions of the load given V and H_s for all the offshore and onshore wind-wave combinations. Using the extreme loads POT data, a three-parameter Weibull fit is applied for each V-H_s bin to yield the short-term distributions.

Figure 5 shows probability of load exceedance curves for onshore, offshore, and all-direction winds. It is clear that offshore winds govern the long-term design loads for almost all return periods. Also, design loads based on the "all-direction" winds are almost the same as those based on the offshore winds. This is because at longer return periods, the exceedance probability (of associated large load levels) for offshore winds is about two orders of magnitude higher than that for onshore winds, and thus the exceedance probability for the all-direction winds is almost same as that for the offshore winds alone.

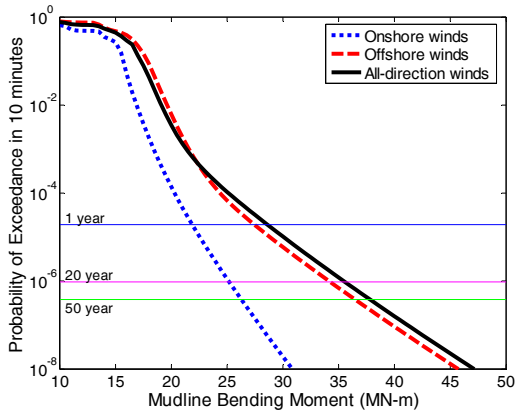

Figure 5: Probability of load exceedance curves for onshore, offshore, and all-direction winds.

Table 3: Comparison of 1- and 20-year design loads (mudline bending moment in MN-m) from this study and from Agarwal and Manuel [4]

Method	Onshore		Offshore		All-direction	
	1-yr	20-yr	1-yr	20-yr	1-yr	20-yr
Present Study (POT-based)	21.9	25.2	27.4	34.3	28.6	35.6
Agarwal and Manuel [4]	23.9	29.7	29.2	37.7	29.4	37.9

The present study was based on the use of campaign data (i.e., time series data) to which the peak-over-threshold method was applied to yield short-term load distributions that were then used with Eq. (1) to yield the curves shown in Fig. 5. In an earlier study, Agarwal and Manuel [4] used summary data from the same Blyth measurements (only global maxima were considered) and similar curves were developed there. Table 3 shows a comparison of 1- and 20-year design loads from the two studies. The present study yields consistently smaller design load levels. However, as is clear from the table, the 1-year loads from the present study, in all cases, were generally never more than 10% smaller and the 20-year loads never more than 15% smaller.

Because the design loads derived as summarized in Fig. 5 and Table 3 are based on the use of limited data, there is uncertainty associated with their estimation. We employ non-parametric bootstrap techniques (Efron and Tibshirani [6]) that rely on randomly resampling with replacement of the POT data and then estimating three-parameter Weibull parameters for the short-term load distributions in Eq. (1). Exceedance probability curves for each of the resamplings are then developed and can yield 5- and 95-percentile levels of probability for a specified load level. These then represent 90-percent confidence intervals as shown in Fig. 6. For instance, from Figs. 5 and 6, one can say that the 20-year mean design load is 35.6 MN-m for the all-direction winds case but that there is a 90-percent chance that the 20-year design load may lie between roughly 29 and 40 MN-m. It is also noted that the confidence intervals for offshore winds are larger than for onshore winds.

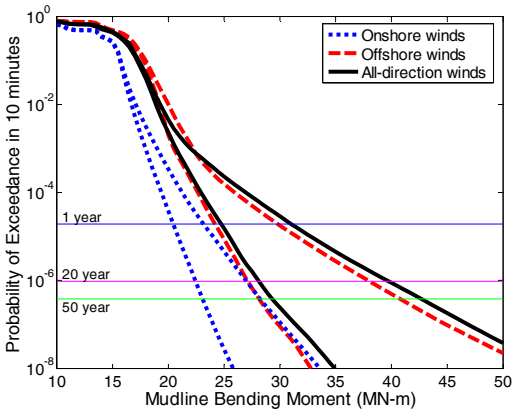

Figure 6: Ninety-percent confidence intervals on probability of load exceedance curves for onshore, offshore, and all-direction winds based on bootstrapping.

CONCLUSIONS

Our objective in this study was to derive long-term design loads for a 2MW offshore wind turbine sited in 9 meters of water at the Blyth site in the United Kingdom. Field data were available on wind speed, wave height, and mudline bending moment. Using time series data on the turbine load, the peak-over-threshold method was applied to develop load distributions given wind speed and wave height for offshore winds (winds blowing from land towards sea) and onshore winds (winds blowing sea towards land). Integration of these distributions along with the relative likelihood of different wind speed and wave height combinations allowed derivation of turbine long-term design loads.

The following represent some general conclusions based on the analyses conducted:

- Offshore winds govern the design loads for the instrumented wind turbine at Blyth. A detailed analysis of available time series shows that offshore winds result in larger loads, compared to onshore winds, due to the larger turbulence intensity associated with offshore winds.
- Waves have only a secondary influence on turbine loads. They can contribute significant amount of energy at frequencies close to the tower natural frequency. Still, even when wave heights are much larger, which is more likely for onshore winds, turbine loads are not as large as for some offshore wind cases since the accompanying turbulence intensity in the wind is much lower.
- Design loads based on the POT method using the campaign data are reasonably close to those based on the global maxima method that were based on the use of summary data.
- Confidence intervals on turbine design loads, obtained using non-parametric bootstrap methods, are larger for offshore winds.

ACKNOWLEDGMENTS

The authors gratefully acknowledge the financial support provided by a CAREER Award (No. CMS-0449128) from the National Science Foundation and by Contract No. 30914 from Sandia National Laboratories. They also thank Garrad Hassan and Partners for providing the data recorded at the Blyth site.

REFERENCES

[1] IEC 61400-3, 2005, Wind Turbines – Part 3: Design Requirements for Offshore Wind Turbines, International Electrotechnical Commission, TC88 WG3 Committee Draft.

[2] Moriarty, P. J., Holley, W. E. and Butterfield, S. P., 2004, Extrapolation of Extreme and Fatigue Loads using Probabilistic Methods, National Renewable Energy Laboratory, NREL/TP-500-34421, Golden, CO.

[3] Fitzwater, L.M. and Winterstein, S.R., 2001, "Predicting Design Wind Turbine Loads from Limited Data: Comparing Random Process and Random Peak Models," Proceedings of the 2001 ASME Wind Energy Symposium, pp. 355-364, Reno, Nevada.

[4] Agarwal, P. and L. Manuel, 2007, On the Joint Wind-Wave Environment and its Influence on Offshore Wind Turbine Loads, Proceedings of the 2007 ASME Wind Energy Symp., Reno, Nevada.

[5] Camp, T.R., et al., 2003, Design Methods for Offshore Wind Turbines at Exposed Sites, Final Report of the OWTES Project, Garrad Hassan and Partners Ltd., Bristol, UK.

[6] Efron, B. and Tibshirani, R.J., 1993, An Introduction to the Bootstrap, Chapman and Hall, New York